European Journal of Radiology 101 (2018) 170–177

Contents lists available at ScienceDirect

European Journal of Radiology

journal homepage: www.elsevier.com/locate/ejrad

Research article

Predictive quantitative sonographic features on classification of hot and cold thyroid nodules

Ali Abbasian Ardakani[a], Ali Mohammadzadeh[b], Nahid Yaghoubi[c], Zahra Ghaemmaghami[d], Reza Reiazi[a,e], Amir Homayoun Jafari[f], Sepideh Hekmat[g], Mohammad Bagher Shiran[a,*], Ahmad Bitarafan-Rajabi[a,c,*]

[a] Department of Medical Physics, School of Medicine, Iran University of Medical Sciences, Tehran, Iran
[b] Department of Radiology, Rajaei Cardiovascular, Medical and Research Center, Iran University of Medical Sciences, Tehran, Iran
[c] Department of Nuclear Medicine, Rajaei Cardiovascular, Medical and Research Center, Iran University of Medical Sciences, Tehran, Iran
[d] Rajaei Cardiovascular, Medical and Research Center, Iran University of Medical Sciences, Tehran, Iran
[e] Medical Image and Signal Processing Research Core, Iran University of Medical Sciences, Tehran, Iran
[f] Department of Medical Physics & Biomedical Engineering, School of Medicine, Tehran University of Medical Sciences, Tehran, Iran
[g] Department of Nuclear Medicine, School of Medicine, Hasheminejad Hospital, Iran University of Medical Sciences, Tehran, Iran

ARTICLE INFO

Keywords:
Computer-assisted
Pattern recognition
Radionuclide imaging
Thyroid nodule
Thyrotropin
Ultrasonography

ABSTRACT

Purpose: This study investigated the potentiality of ultrasound imaging to classify hot and cold thyroid nodules on the basis of textural and morphological analysis.
Methods: In this research, 42 hypo (hot) and 42 hyper-function (cold) thyroid nodules were evaluated through the proposed method of computer aided diagnosis (CAD) system. To discover the difference between hot and cold nodules, 49 sonographic features (9 morphological, 40 textural) were extracted. A support vector machine classifier was utilized for the classification of LNs based on their extracted features.
Results: In the training set data, a combination of morphological and textural features represented the best performance with area under the receiver operating characteristic curve (AUC) of 0.992. Upon testing the data set, the proposed model could classify the hot and cold thyroid nodules with an AUC of 0.948.
Conclusions: CAD method based on textural and morphological features is capable of distinguishing between hot from cold nodules via 2-Dimensional sonography. Therefore, it can be used as a supplementary technique in daily clinical practices to improve the radiologists' understanding of conventional ultrasound imaging for nodules characterization.

1. Introduction

A thyroid nodule can be formed as a result of the growth of an abnormal cell within the thyroid gland which may appear as a non-palpable or palpable mass. According to the national cancer institute, 56.870 new cases and 2.010 thyroid cancer related deaths occurred in 2017. There has been an increase in death rates at an average rate of 0.7% each year over 2005–2014 [1]. Serum thyrotropin (TSH) should be obtained as an initial evaluation process from all patients diagnosed with a thyroid nodule. For patients with a subnormal TSH level, before any further diagnostic procedures like fine needle aspiration (FNA), a radionuclide thyroid scan should be performed. The scan result can be hyperfunctioning (hot), isofunctioning (warm) or nonfunctioning (cold) (i.e., tracer uptake is less, equal or greater than the surrounding normal thyroid tissue respectively). Although hot nodules rarely represent malignancy, 3–15% of cold nodules have been reported as malignant [2–4]. Therefore, radionuclide scan plays a critical role in the evaluation of thyroid nodule in patients with low TSH level. For other cases with high TSH level, FNA should be performed due to the high risk of malignancy [3].

According to the American Thyroid Association (ATA), ultrasound is the main and preferred imaging modalities for thyroid nodule evaluation, while if a thyroid nodule is detected incidentally on any other imaging modalities, for more assessment ultrasonography should be performed [3]. An ultrasound image reflects diverse gray-level intensities and different tissues have different textures. Although there is no precise or mathematical definition of texture, it is simply conceived by the human eye. Image texture can be described by spatial variations in pixel intensity, patterns (homogen or heterogen, smooth, or coarse) of objects within an image. In other words, different patterns of echo

* Corresponding authors at: Department of Medical Physics, School of Medicine, Iran University of Medical Sciences, Tehran, Iran. Tel/fax: +98 21-886-22647.
E-mail addresses: shiran.m@iums.ac.ir, A.atrdekani@live.com (M.B. Shiran), Bitarafan@rhc.ac.ir (A. Bitarafan-Rajabi).

https://doi.org/10.1016/j.ejrad.2018.02.010
Received 12 January 2018; Received in revised form 4 February 2018; Accepted 9 February 2018

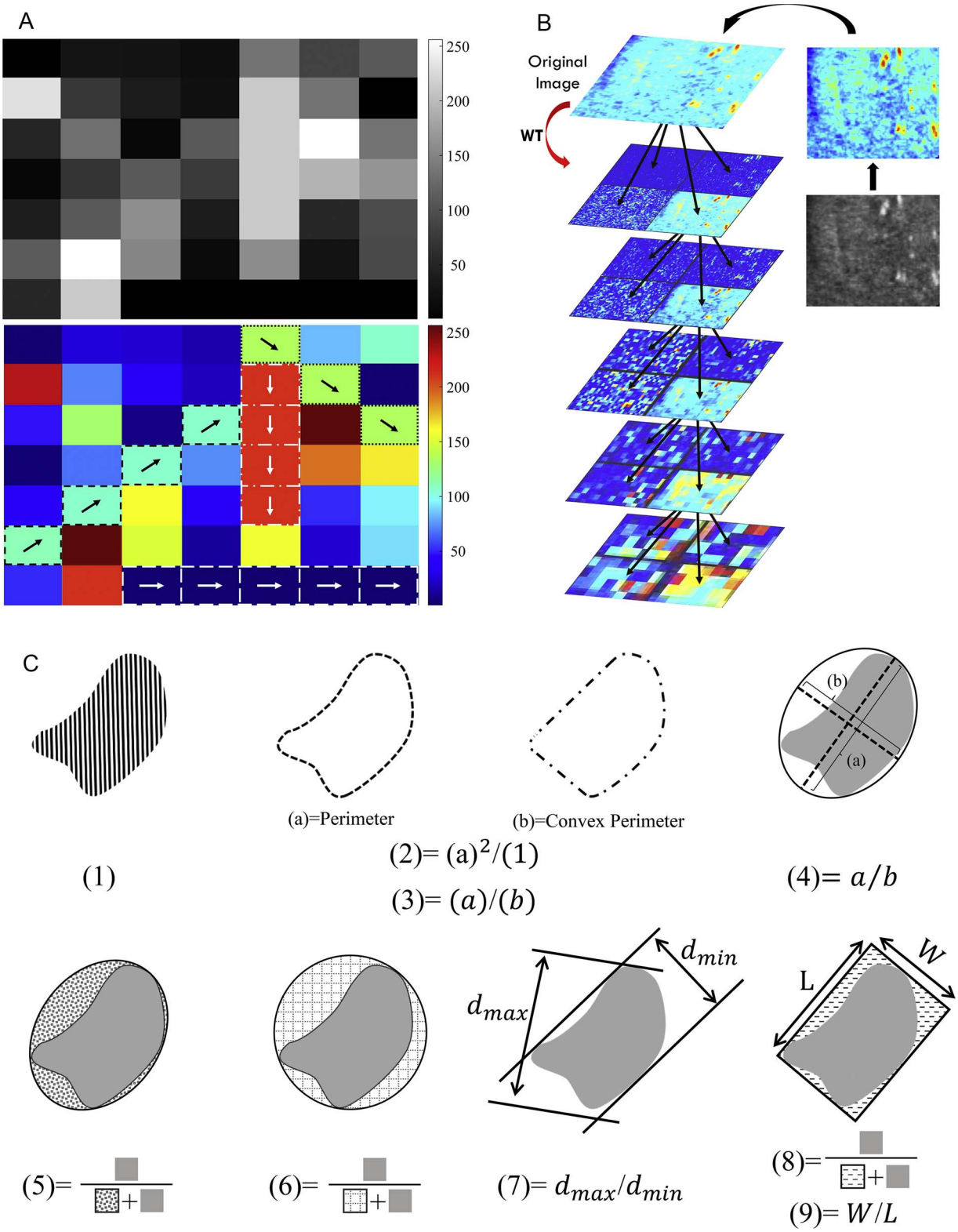

Fig. 1. Three quantitative groups were used in this study: (A), Run-length matrix: the arrows indicate the direction of runs of pixels having the same value; (B), Wavelet: features computed at five decomposition levels; and (C), Morphological based features.

from a nodule can form different textures within an ultrasound image. The structural abnormalities of a thyroid nodule are capable of representing different textures that can be extracted by visual inspection, but complex patterns are difficult to interpret [5,6].

Although radionuclide scan is the standard method for evaluation of a thyroid nodules function, its invasive, incurs health care costs and imposes anxiety and radiation doses on the patient [7]. Today, computer-aided diagnosis (CAD) systems have become an important part of clinical duty routines to help and improve the accuracy of an initial radiologist's diagnosis. CAD systems have an advantage over humans due to overcoming the limitations of human memory, fatigue, reproducibility and ability to detect pathological changes that cannot be

detected by the human eye [6,8]. Recently, CAD systems have been proposed for thyroid nodules characterization in ultrasound imaging. Many quantitative sonographic features such as morphology [9–12], texture [10,13–18], and elastography [15,19,20] have been shown to be useful in differentiating between benign and malignant thyroid nodules. The present study provides additional information relevant to the possibility of ultrasound imaging in distinguishing hot from cold nodules. To the best of the authors' knowledge, no published studies have evaluated the potential of ultrasound imaging or other imaging modalities, for the classification of hot and cold thyroid nodules.

2. Patients and methods

2.1. Patients and image acquisition

Data were obtained from patients who had undergone radionuclide thyroid scan at the Rajaie cardiovascular medical and research center. Each patient provided written informed consent, and a local ethics committee approval was obtained for this prospective study.

The inclusion criteria were as follows: Patients who had nodules with a length greater than 10 mm in diameter, Patients who had been tested for serum TSH and Patients with TSH suppression level (< 0.5 μIU/mL). The following were excluded from the study: patients who recently had a myocardial infarction (MI), congestive heart failure (CHF) and surgery, who recently received contrast agent, amiodarone and pregnancy within the previous six months, who are suspected of having thyroiditis, who had more than one nodule with a diameter larger than 10 mm and individuals who refused to sign the consent form.

Neck ultrasonography was performed on these patients as a routine evaluation just before radionuclide thyroid scan. Ultrasonography was performed using the IU22 sonography system (Philips Healthcare, Bothell, Washington, USA) equipped with a L12-5 (5–12 MHz) linear array transducer. To select the biggest cross section, all detected nodules were evaluated in longitudinal and transverse sections. For further evaluation, only one image per nodule with the maximum cross section was used. For further analysis, all ultrasound thyroid nodules were labeled according to the radionuclide scan result.

In this study, a radionuclide thyroid scan was acquired using Infinia Hawkeye 4 SPECT-CT (GE Medical Healthcare, Milwaukee, WI, USA) equipped with a low-energy general propose (LEGP), parallel-hole collimator with matrix size of 256*256 and zoom factor of 2. Imaging was done 20 min after intravenous administration of 4 mCi ^{99m}Tcpertechnetate for 180 s (700–1000k counts per view). The 20% symmetric window was centered on the^{99m}Tc140 keV photopeak. To remove the confounder factor, all patients stopped taking Methimazole for one week before the radionuclide thyroid scan.

2.2. Nodule segmentation and quantitative features extraction

2.2.1. Nodule segmentation

In our previous study, hybrid filter was introduced for thyroid nodules segmentation in ultrasound imaging. This hybrid filter contains 4 layers: 1-contrast limited adaptive histogram equalization (CLAHE); 2-wavelet filter in “high-high” frequency channel in second level wavelet decomposition (WletHH2); 3-probabilistic patch-based (PPB) filter and 4- Homomorphic WletHH2 (Hmp_WletHH2) filter. Through the application of the hybrid filter, active contour can segment a thyroid nodule with high performance and the area under the receiver operating characteristic (ROC) curve (AUC) was 0.943. In the present study, the proposed segmentation method is applied to the nodule segmentation to prepare the region of interest for further features extractions.

2.2.2. Texture features

2.2.2.1. Run length matrix. In some sonographic patterns, some pixels with same gray-level intensity was continuous in a specific direction. The run length matrix (RLM) based features can describe these distributions. In other words, RLM p(i, j) represent runs of length j of pixels having the same gray-level value i in the nodule region (Fig. 1A). In this regards, five quantitative features were calculated from RLM: 1-run length nonuniformity (RLNU), 2- gray level nonuniformity (GLNU), 3- short run emphasis (SRE), 4- long run emphasis (LRE), and 5-fraction of the image in runs (Fraction). Each of these five features are calculated in four directions: vertical, horizontal, 45°, and 135°. Hence, twenty RLM texture features were included in this study.

2.2.2.2. Wavelet. Wavelet is a robust technique for texture analysis due to the analysis and localized natural nonstationary signals in both spatial and frequency domains. Wavelet can decompose the signal of an image into successive levels using independent spatially oriented frequency channels in a pyramidal structure. In this regards, sets of high-pass (H) and low-pass (L) filters are employed to increase frequency resolution and produce wavelet coefficients at each level and direction. In each decomposition level, filters were applied for all rows (horizontal direction) and then for all columns (vertical direction) of an image. Hence, at n-th decomposition levels, the output contained four different subband images with their corresponding wavelet coefficients given in parentheses: one approximation subband image (a^n_{LL}) and sets of detailed subband images (d^n_{HH}, $d^n_{HL}$and d^n_{LH}). The a^n_{LL} is used for further transformation at the next levels (Fig. 1B). The energy of each of these wavelet coefficients are measured as follows:

$$E^n_{sub-band} = \frac{\sum_{i,j\varepsilon ROI} (d_{sub-band;i,j})^2}{N}$$

Where E and N denote energy and number of pixel in ROI [13]. In this study, the energy of wavelet coefficients at five levels were computed. Hence, 20 wavelet features were used for texture analysis (Fig. 1B).

2.2.3. Morphological features

Based on literature, there is a difference in the morphology of benign and malignant thyroid nodules. Generally, a malignant nodule has an irregular margin, taller-than-wide shape, smaller size and greater Aspect_Ratio [11,12,21–23]. The study hypothesis is that there may be some variations in morphological features between hot and cold thyroid nodules. After nodule segmentation, various morphological parameters can be calculated. In this study, nine morphological parameters were calculated to find the differences between hot and cold nodules. These nine parameters included the following: 1- Area: return number of pixels within nodule, 2- Compactness: the ratio of perimeter square (perimeter^2) to area of nodule, 3- Convexity: the ratio of perimeter to convex perimeter of nodule (convex perimeter defined as perimeter of smallest convex polygon that can contain nodule), 4- Extent: the ratio of major to minor axis length of the ellipse that circumscribe the nodule, 5- Ellipticity: the ratio of the nodule area to the area of the ellipse which circumscribe the nodule, 6- Circularity: the ratio of the area of the nodule to the area of the circle that circumscribe the nodule, 7- Aspect_ratio: the ratio of the maximum to the minimum diameter of the nodule, 8- Form_factor: the ratio of the nodule area to the bounding box area, and 9- Square_factor: the ratio of the width to the length of the circumscribed rectangle of the nodule. Fig. 1C presents an illustration of these morphological parameters.

2.3. Statistical analysis and classification

All quantitative data were tested for normality by the Kolmogorov–Smirnov test. The two tailed independent samples *t*-test/Mann–Whitney *U* test were applied for comparisons of quantitative parameters between hot and cold nodules. The sex distribution between the two groups, was evaluated using Fisher's exact and Chi square tests. A P-value less than 0.05 was considered significant.

Support vector machine (SVM) uses all significant quantitative features to classify the two groups. SVM is an interesting and powerful supervised machine learning approach for data classification and modeling. SVM defines optimal hyperplane with maximum margin by using labeled training data and support vectors from feature space. In this condition, new data can be categorized according to hyperplane [24]. After training and creating the SVM model, new samples can be assigned into one category. In addition to linear classification, SVM can solve a non-linear problem using a "kernel trick". In this technique, the feature space was mapped into a higher dimension to provide a linear classification. Cross-validation testing is a useful method to prevent over-fitting and to improve classifier generalizability. The 10-fold cross-validation is used for model building. In this case, feature parameters are randomly divided into 10 folds with equal size. Thereafter, nine folds are used for training data and one fold is used for testing. This procedure is continued while all folds are used for testing. Almost 70% of patients (with 50–50 distribution) were randomly selected for training and other 30% of the patients (with 50–50 distribution) were used as a new and blind data to test the final model.

To compare diagnostic performances, five well-known indexes were calculated: accuracy (ACC), sensitivity (SEN), specificity (SPC), positive predictive value (PPV), and negative predictive value (NPV). In this study, hot and cold nodules were considered as negative and positive cases, respectively. The AUC was also calculated to evaluate the overall performance of the proposed method [25]. ROC analysis was performed using the SPSS software (IBM SPSS Statistics 19 for Windows, IBM Inc., Armonk, NY, USA) and AUC values were estimated beyond the 95% confidence level. The steps of the proposed CAD process are presented in Fig. 2.

3. Results

3.1. Demographic data of patients

In this study, 84 patients (51 female, 33 male) with proven radionuclide scan results were considered. Of these 84 patients, hyper-functioning nodules (hot nodules) existed in 42 patients (25 female, 17 male) and 42 patients (26 female, 16 male) had only hypo-functioning nodules (cold nodules). There was no significant difference between hot and cold nodules in terms of gender (p = 0.823). Also, the mean age (mean ± SD) of the hot and cold groups were 51.67 ± 13.41 and 54.55 ± 12.43 respectively, but the difference did not reach a level of significance (P = 0.310). Since the differences in gender and age of patients between the two groups (hot and cold) were not statistically significant, these parameters were not determined as confounding factors in quantitative extracted features from images. All patients with cold thyroid nodules underwent the FNA and positive FNA results were found in 8 patients (5 female and 3 male).

Out of 84patients, 60patients (30 hot and 30 cold nodules) were randomly selected for training and the other 24 patients (12 hot and 12 cold nodules) were taken as the new and blind data for testing the final model. Fig. 3 shows the sample ultrasound image of hot and cold nodules with the corresponding scintigraphic image.

3.2. Distributions of textural and morphological features in the two groups

Table 1 presents the distribution characteristics of quantitative features in patients. Fig. 4A–C presents the ROC curves of the individual features. From all 40 textural features, there were 25 significant differences between hot and cold nodules. In this case, GLNU in the horizontal direction (Horz_GLNU), Horz_LRE, Horz_SRE and Horz_Fraction, RLNU in the vertical direction (Vert_RLNU), Vert_GLNU, Vert_SRE and Vert_Fraction, RLNU in 45° direction (45Dgr_RLNU), 45Dgr_GLNU, 45Dgr_SRE and 45Dgr_Fraction, RLNU in 135° direction (135Dgr_RLNU), 135Dgr_GLNU, 135Dgr_SRE and 135Dgr_Fraction form RLM features; and "low-high" energy components in the first level wavelet decomposition (WavEnLH_s-1), "high- low" energy components in the first, second, 3rd, 4th and 5th level wavelet decomposition (WavEnHL_s-1, WavEnHL_s-2, WavEnHL_s-3, WavEnHL_s-4, and WavEnHL_s-5), "high- high" energy components in the first, second, 3rd and 5th level wavelet decomposition (WavEnHH_s-1, WavEnHH_s-2, and WavEnHL_s-3) from wavelet are significant features (Table 1). Table 1 presents the mean value of all significant features in hot and cold groups.

It was found that among the nine morphological features, only Compactness and Form_factor did not have any significant difference between hot and cold nodules. Seven significant features are as follows: Area, Convexity, Extent, Ellipticity, Circularity, Aspect_ratio and Square_factor (Table 1).

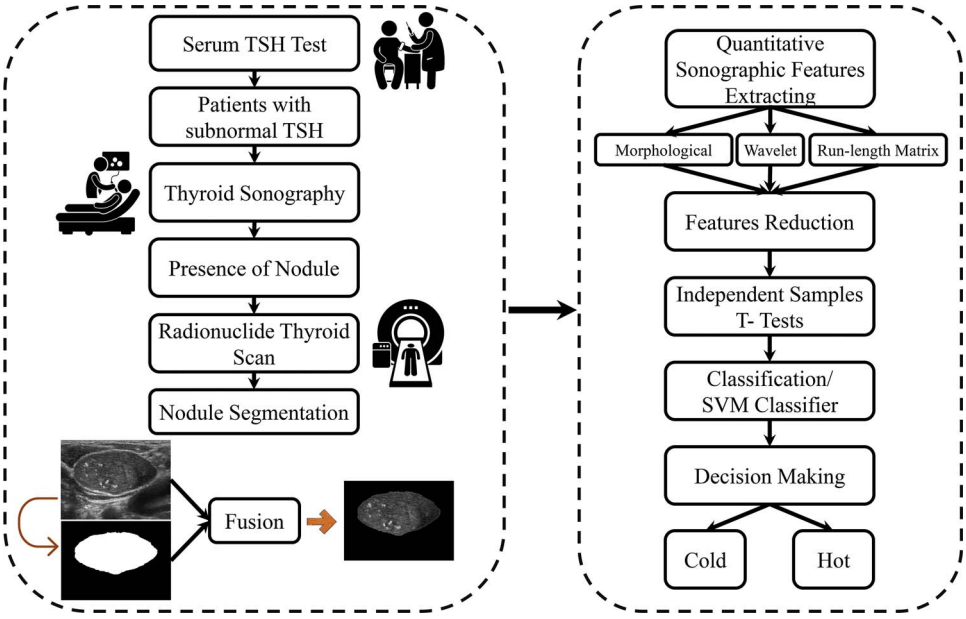

Fig. 2. Overview of proposed method process on ultrasound images.

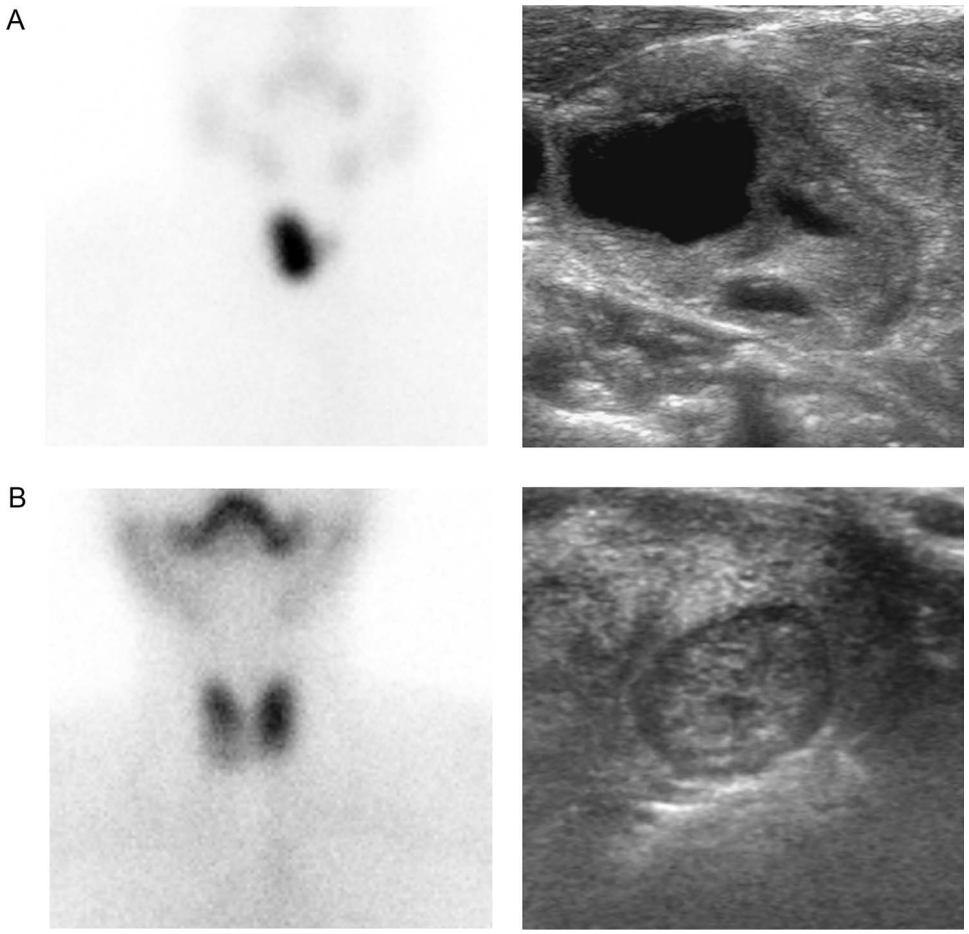

Fig. 3. Sample image of (A) hot and (B) cold nodule Scintigraphic and their corresponding ultrasound images were located at top and bottom of figure.

3.3. Classification performance between hot and cold nodules

Using SVM, the all significant features between the two groups were implemented for multi-parameter analysis. Table 2 shows the diagnostic performance of SVM for classifying and making comparisons between hot and cold nodules for each feature type and the combination with each other. Also, Fig. 4D presents the ROC curves of the SVM model on the same graph for each feature groups so as to compare the discriminating power of classification.

Considering the feature classes, textural features can lead to AUC of 0.943 which corresponds to 93.33% sensitivity, 96.67% specificity and 95.00% accuracy in the classification of hot and cold nodules. Morphological features can distinguish hot from cold nodules with AUC of 0.885, corresponding to sensitivity of 86.67%, specificity of 90% and accuracy of 88.33%. The combination of morphological and textural feature groups represented the highest performance in terms of AUC, sensitivity, specificity and accuracy of 0.992, 100%, 96.67% and 98.33% respectively.

After 10-fold cross-validation, the final model was tested with 24 new cases (12 hot and 12 cold) represents high performance with AUC of 0.948 which corresponds to sensitivity, specificity and accuracy of 91.67%.

4. Discussion

To improve the accuracy of physician's initial diagnoses and therapy, discriminating between hot and cold thyroid nodules is regarded as one of the most critical factors. The primary objective of this study was to evaluate the morphological and textural sonographic features ability, a non-invasive method for identifying changes between hot and cold thyroid nodules. The results of the current study proved that the proposed CAD system can differentiate between hot and cold thyroid nodules with high accuracy.

The results showed that the combination of morphological and textural features had more discriminative power than those features alone according to the AUC (combination vs. textural vs. morphological features: 0.992 vs. 0.943 vs. 0.885). It can be concluded that these two feature classes are complementary and their fusion can improve the performance of the classification task. Hence, in the data of this research, where the best results were driven in combination features with an AUC of 0.992 which corresponds to a sensitivity of 100%, a specificity of 96.67% and accuracy of 98.33%. Testing the final validated model indicated that this model can classify blind hot and cold nodules with high performance with AUC of 0.948, sensitivity, specificity and accuracy of 91.67%.

Since the last decade, the CAD system has been employed for the classification of benign and malignant thyroid nodules using ultrasound imaging. No study has been found with the aim of classifying hot and cold nodules. Ultrasound imaging includes many kinds of features, such as textural, elastographic and morphological features which are useful for classification tasks. Through histogram and gray-level co-occurrence matrix (COM) features, Kim et al. [15] was able to classify benign and malignant thyroid nodules with AUC 0f 0.809. In order to distinguish between benign and malignant thyroid nodules, RLM and COM were extracted by Chang et al. [16] this resulted to an accuracy of 83.10% for both texture groups. Acharya et al. [17] employed Gabor transform to extract quantitative texture feature for classification of benign and malignant thyroid nodules. In this regard, 94.3% accuracy was achieved. Also, in our previous studies, benign and malignant thyroid nodules were classified with AUC of 1 and 0.9722 by using wavelet and

Table 1
Main textural and morphological characteristics data of hot and cold thyroid nodules.

Group	Parameter	Hot Mean ± SD	Cold	P-value	AUC
RLM	Horz_RLNU	7531.618 ± 1181.667	9726.842 ± 1208.318	0.199	–
	Horz_GLNU	642.268 ± 93.135	1149.612 ± 137.871	0.003	0.726 (0.582, 0.869)
	Horz_LRE	2.931 ± 0.330	5.738 ± 0.546	< 0.001	0.860 (0.764, 0.956)
	Horz_SRE	0.793 ± 0.007	0.688 ± 0.014	< 0.001	0.877 (0.793, 0.960)
	Horz_Fraction	0.718 ± 0.011	0.5761 ± 0.016	< 0.001	0.888 (0.803, 0.972)
	Vert_RLNU	9731 ± 1494.621	19752.416 ± 2443.191	0.002	0.733 (0.591, 0.876)
	Vert_GLNU	717.846 ± 103.461	1610.684 ± 202.203	< 0.001	0.749 (0.610, 0.888)
	Vert_LRE	2.049 ± 0.148	2.529 ± 0.278	0.133	–
	Vert_SRE	0.852 ± 0.005	0.832 ± 0.007	0.022	0.702 (0.561, 0.844)
	Vert_Fraction	0.800 ± 0.009	0.768 ± 0.010	0.023	0.700 (0.557, 0.843)
	45Dgr_RLNU	10510.044 ± 1595.274	21017.426 ± 2583.022	0.001	0.730 (0.588, 0.872)
	45Dgr_GLNU	738.833 ± 105.586	1656.793 ± 206.955	< 0.001	0.752 (0.614, 0.891)
	45Dgr_LRE	1.842 ± 0.127	2.292 ± 0.209	0.071	–
	45Dgr_SRE	0.871 ± 0.004	0.8431 ± 0.006	0.001	0.761 (0.628, 0.895)
	45Dgr_Fraction	0.827 ± 0.008	0.786 ± 0.009	0.001	0.757 (0.619, 0.895)
	135Dgr_RLNU	10548.807 ± 1602.631	21055.906 ± 2581.413	0.001	0.729 (0.587, 0.871)
	135Dgr_GLNU	741.193 ± 106.185	1655.882 ± 207.096	0.001	0.751 (0.612, 0.890)
	135Dgr_LRE	1.826 ± 0.116	2.264 ± 0.204	0.067	–
	135Dgr_SRE	0.871 ± 0.005	0.844 ± 0.006	0.001	0.753 (0.616, 0.890)
	135Dgr_Fraction	0.828 ± 0.008	0.787 ± 0.009	0.001	0.744 (0.604, 0.885)
Wavelet	WavEnLL_s-1	7109.997 ± 402.655	6134.101 ± 437.337	0.106	–
	WavEnLH_s-1	19.644 ± 1.222	14.883 ± 1.355	0.004	0.714 (0.576, 0.849)
	WavEnHL_s-1	7.650 ± 0.4150	3.394 ± 0.334	< 0.001	0.904 (0.837, 0.972)
	WavEnHH_s-1	1.654 ± 0.156	0.707 ± 0.161	< 0.001	0.824 (0.701, 0.948)
	WavEnLL_s-2	7069.448 ± 401.043	6080.988 ± 433.867	0.100	–
	WavEnLH_s-2	33.252 ± 1.431	29.794 ± 2.016	0.167	–
	WavEnHL_s-2	15.556 ± 1.001	8.280 ± 0.724	< 0.001	0.874 (0.786, 0.963)
	WavEnHH_s-2	5.792 ± 0.400	2.583 ± 0.320	< 0.001	0.877 (0.786, 0.968)
	WavEnLL_s-3	7043.601 ± 396.721	6031.438 ± 433.873	0.090	–
	WavEnLH_s-3	43.069 ± 2.374	43.632 ± 2.901	0.881	–
	WavEnHL_s-3	20.240 ± 1.273	15.497 ± 1.377	0.014	0.699 (0.563, 0.834)
	WavEnHH_s-3	10.612 ± 0.998	8.755 ± 1.253	0.001	0.746 (0.613, 0.878)
	WavEnLL_s-4	6004.900 ± 437.584	7035.548 ± 400.673	0.088	–
	WavEnLH_s-4	47.331 ± 2.926	47.054 ± 5.062	0.433	–
	WavEnHL_s-4	25.662 ± 1.580	19.615 ± 1.711	0.012	0.674 (0.538, 0.811)
	WavEnHH_s-4	9.889 ± 0.680	9.759 ± 0.901	0.909	–
	WavEnLL_s-5	7028.542 ± 382.304	6193.617 ± 491.928	0.185	–
	WavEnLH_s-5	58.127 ± 6.123	102.671 ± 28.198	0.657	–
	WavEnHL_s-5	36.194 ± 3.462	25.456 ± 3.283	0.005	0.713 (0.682, 0.844)
	WavEnHH_s-5	13.170 ± 0.884	11.491 ± 1.199	0.264	
Morphology	Area	56614.467 ± 15174.938	66493.567 ± 19390.619	0.032	0.659 (0.518, 0.799)
	Compactness	103.867 ± 8.143	106.6784 ± 8.432	0.160	–
	Convexity	2.326 ± 0.134	2.574 ± 0.132	< 0.001	0.889 (0.809, 0.969)
	Extent	1.466 ± 0.114	1.547 ± 0.148	0.021	0.682 (0.544, 0.821)
	Ellipticity	0.631 ± 0.052	0.696 ± 0.095	0.012	0.689 (0.552, 0.825)
	Circularity	0.609 ± 0.062	0.524 ± 0.067	< 0.001	0.814 (0.707, 0.922)
	Aspect_ratio	1.323 ± 0.136	1.808 ± 0.395	< 0.001	0.890 (0.818, 0.961)
	Form_factor	0.735 ± 0.085	0.756 ± 0.071	0.315	–
	Square_factor	1.239 ± 0.128	1.738 ± 0.329	< 0.001	0.861 (0.812, 0.890)

combination groups of texture features, respectively [13,14].

Ultrasound elastography is a non-invasive technique, capable of displaying tissue deformation caused by compression [26]. Furthermore, in several studies, ultrasound elastography has been used to classify benign and malignant thyroid nodules. Through real-time elastography, Sui et al. [19] were able to assess stiffness and classify benign and malignant thyroid nodules with a sensitivity, specificity, accuracy and AUC of 88.30%, 88.37%, 83.49%, and 0.863 respectively. Zhang et al. [20] were able to assess stiffness by using strain elastography, virtual touch tissue imaging and acoustic radiation force impulse (ARFI) Imaging. They indicated that thyroid nodules, after measuring shear-wave velocity (SWV) from ARFI imaging, can be classified with higher performance of which AUC, sensitivity, specificity, and accuracy were 0.869, 78.18%, 83.51%, and 81.58%, respectively.

Margin irregularity, symmetry, as well as the surface shape of a thyroid nodule are described by morphological features. In this regard, Sui et al. [19] indicated that malignant nodules have higher aspect ratio compared to benign nodules ($P < 0.001$). However, there was no difference between the nodules in terms of margin regularity ($P = 0.329$). On the other hand, Ma et al. [11] achieved the opposite result. They showed that margin irregularity as well as oval shape are more common in malignant nodules with 84% Sensitivity and 66.7% specificity ($P < 0.05$). Also Xia et al. [27] proved that irregular margin was more common in malignant nodules ($P < 0.001$). In Wu et al.'s study [12], benign nodules were significantly larger than malignant nodules but taller-than-wide shape was more common in malignant nodules. Also Nam et al. [28] indicated that parallel shapes are more common in benign nodules compared to malignant nodules ($P < 0.001$).

The aforementioned studies aimed to diagnose benign and malignant thyroid nodules. But no study has tested the validity of imaging modalities in the diagnosis of hot from cold nodules. However, for the first time, in the present study, the differences between hot and cold thyroid nodules were analyzed through the use of quantitative sonographic features. Consequently, a good classification was presented by these features. Accordingly, radionuclide thyroid imaging can be avoided in patients with uncertain nodule function, if this model is utilized for their diagnoses.

In textural features groups in order to AUC, wavelet features had a

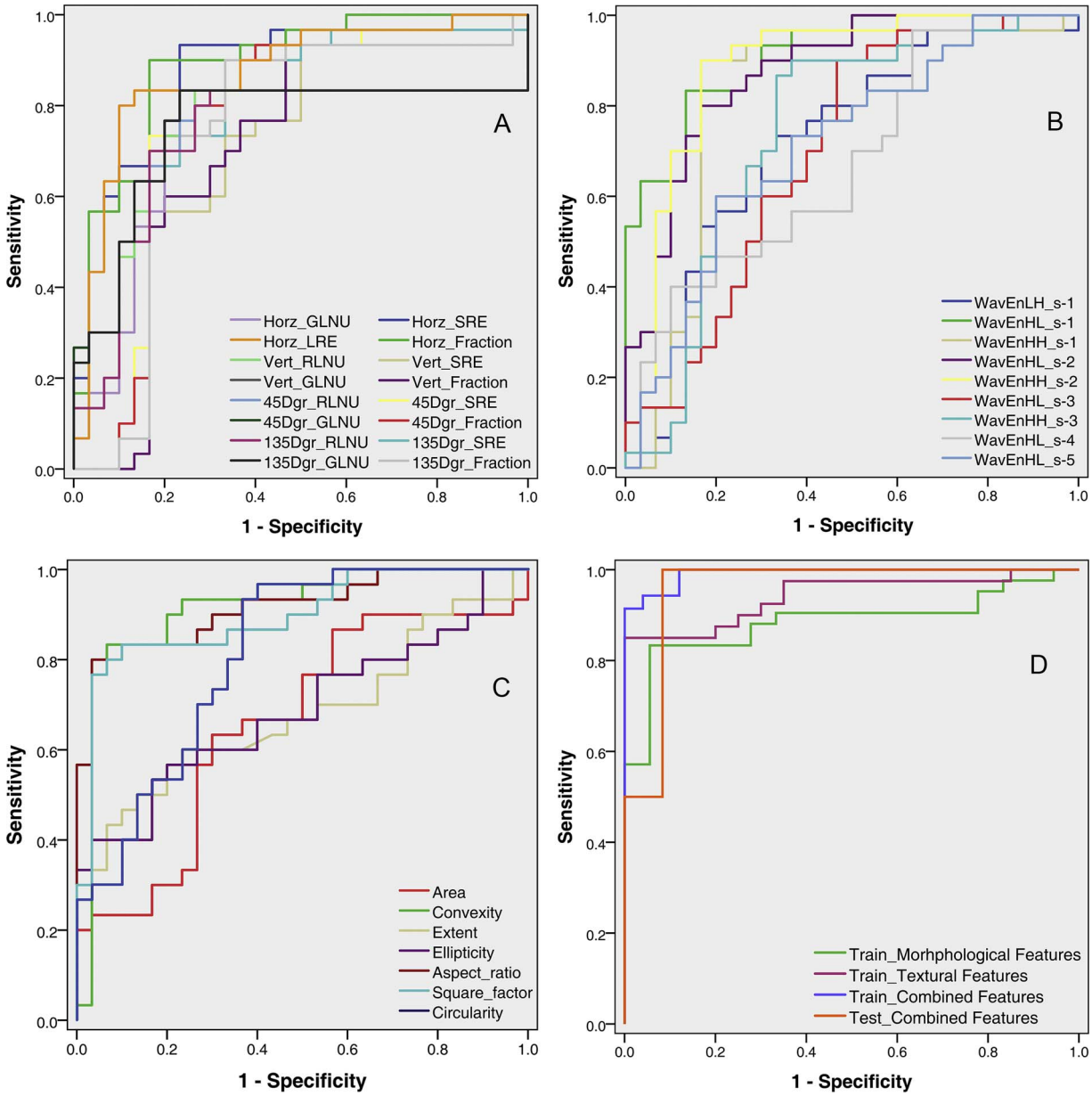

Fig. 4. ROC curves of individual Run-length matrix (A); Wavelet (B); Morphological based features (C) and combination features (D).

higher performance than the RLM features to characterize hot and cold nodules. The values of the best features in wavelet and RLM features were 0.904 (WavEnHL_s-1) and 0.888 (Horz_Fraction), respectively. From the nine morphological features extracted in this study, Area evaluates the size of nodules, Compactness and Convexity measured the irregularity of nodule boundaries; Extent, Aspect_ratio, Form_factor and Square_factor described the extension of nodule shape, while Ellipticity and Circularity measure the roundness of nodules. Consequently, hot nodules have a circular shape and smaller area, while cold nodules have an irregular boundary, higher extent value and an oval shape. In assessing boundary irregularity, Convexity has higher accuracy than Compactness while there was no significant difference between hot and cold nodules in the term of Compactness but Convexity reached a significant level. One of the main reasons for this is that in Convexity parameter, two perimeter and convex perimeter were compared. This can lead to the monitoring of irregularity with the highest accuracy.

Table 2
Diagnostic performance of the proposed multi parameter analysis for classification of hot and cold thyroid nodules.

Groups		SEN(%)	SPC(%)	ACC(%)	PPV(%)	NPV(%)	AUC value[a]	Correct Classification
Train	Textural Features	93.33	96.67	95	96.55	93.55	0.943 (0.886, 0.999)	57/60 [95.00%]
	Morphological Features	86.67	90	88.33	89.65	87.1	0.885 (0.799, 0.971)	53/60 [88.33%]
Test	Morphological + Texture Features	100	96.67	98.33	96.67	100	0.992 (0.978, 1.000)	59/60 [98.33%]
		91.67	91.67	91.67	91.67	91.67	0.948 (0.874, 1.000)	22/24 [91.67%]

SEN = sensitivity; SPC = specificity; ACC = accuracy; PPV = positive predictive value; NPV = negative predictive value; A_z = area under ROC curve.
[a] Numbers in parentheses are 95% confidence intervals.

Hence, for further morphological mass analysis especially in the breast, lymph node and thyroid, Convexity is recommended instead of Compactness for evaluating irregularity of boundaries.

^{99m}Tc, ^{131}I and ^{123}I are useful radionuclides for thyroid gland imaging. Although iodine radionuclide is the main radionuclide for thyroid scintigraphy, it is expensive and of low availability (because it is generated by cyclotron). In this way, ^{99m}Tc is introduced as an analogue of iodine for thyroid imaging. It has been shown that there is no significant difference in the information provided between ^{99m}Tc and ^{123}I. It also had lower radiation dose compared to iodine radionuclide (^{99m}Tc vs. ^{123}Ivs. ^{131}I: 0.013mSv vs. 1.9mSv vs. 6.6mSv) [7]. Hence, in this study, ^{99m}Tc was used for thyroid gland imaging and referencing for thyroid sonography. Also, according to the "as low as reasonably achievable" (ALARA) principle, it is desirable to reduce unnecessary patient's radiation dose as much as possible. The results of this study can help the ALARA principle and indicated that quantitative sonographic features have high potential to distinguish hot from cold thyroid nodules. Also, ultrasonography is the first and primary preoperative choice that can provide adequate information for nodule evaluation. Other imaging modalities such as CT and MRI are used just to insure local invasion degree that can switch or preclude the operative approach [29]. In addition, ultrasonography has an advantage over all other imaging modalities because it has the potential to evaluate nodule malignancy (CT/MRI cannot), is an objective procedure (Elastography is not), low cost (elastography, CEUS, CT, MRI and PET is expensive), radiation free (CT, PET and scintigraphy impose radiation dose) and has high availability (CEUS, Elastography and PET is not routine in clinical centers) [30]. The present results proved that ultrasonography more than ever, is a powerful modality and can monitor thyroid nodule function.

The main advantage of the proposed method is that no additional time, radiation dose and costs are required in the diagnosis process. Patients with warm (isofunctioning) nodules were excluded in this study. Further investigations should be conducted with all types of nodule functioning.

5. Conclusions

In conclusion, a CAD approach to the assessment of hot and cold thyroid nodules on 2-Dimensional sonography was proposed based on textural and morphological features. The preliminary results indicated the usefulness of quantitative features of conventional ultrasound imaging for the characterization of thyroid nodule function as an auxiliary tool during radionuclide thyroid scan in daily clinical practices.

Ethical approval

Informed consent was obtained from all individual participants included in the study. This study was approved by the ethics committee of the Iran University of Medical Sciences (No. IR.IUMS.REC 1395.95-04-30-29762).

Conflicts of interest

None.

Acknowledgement

The current study was a part of PhD thesis which supported by Iran University of Medical Sciences (IUMS).

References

[1] National Cancer Institute. Thyroid cancer—for patients. National Cancer Institute website. http://www.cancer.gov/cancertopics/types/thyroid, in.
[2] S. Garberoglio, O. Testori, Role of nuclear medicine in the diagnosis of benign thyroid diseases, Front. Hormone Res. 45 (2016) 24–36.
[3] B.R. Haugen, E.K. Alexander, K.C. Bible, G.M. Doherty, S.J. Mandel, Y.E. Nikiforov, F. Pacini, G.W. Randolph, A.M. Sawka, M. Schlumberger, 2015, American Thyroid Association management guidelines for adult patients with thyroid nodules and differentiated thyroid cancer: the American Thyroid Association guidelines task force on thyroid nodules and differentiated thyroid cancer, Thyroid 26 (1) (2016) 1–133.
[4] H. Gharib, E. Papini, J.R. Garber, D.S. Duick, R.M. Harrell, L. Hegedüs, R. Paschke, R. Valcavi, P. Vitti, American Association of Clinical Endocrinologists, American College of Endocrinology, and Associazione Medici Endocrinologi Medical Guidelines for clinical practice for the diagnosis and management of thyroid nodules–2016 update, Endocr. Pract. 22 (1) (2016) 1–60.
[5] G. Castellano, L. Bonilha, L.M. Li, F. Cendes, Texture analysis of medical images, Clin. Radiol. 59 (12) (2004) 1061–1069.
[6] B. van Ginneken, C. Schaefer-Prokop, M. Prokop, Computer-aided diagnosis: how to move from the laboratory to the clinic, Radiology 261 (3) (2011) 719–732.
[7] R. Czepczyński, Nuclear medicine in the diagnosis of benign thyroid diseases, Nucl. Med. Rev. 15 (2) (2012) 113–119.
[8] A.A. Ardakani, A. Gharbali, Y. Saniei, A. Mosarrezaii, S. Nazarbaghi, Application of texture analysis in diagnosis of multiple sclerosis by magnetic resonance imaging, Glob. J. Health Sci. 7 (6) (2015) 68–78.
[9] Y.J. Choi, J.H. Baek, H.S. Park, W.H. Shim, T.Y. Kim, Y.K. Shong, J.H. Lee, A computer-aided diagnosis system using artificial intelligence for the diagnosis and characterization of thyroid nodules on ultrasound: initial clinical assessment, Thyroid 27 (4) (2017) 546–552.
[10] Q. Yu, T. Jiang, A. Zhou, L. Zhang, C. Zhang, P. Xu, Computer-aided diagnosis of malignant or benign thyroid nodes based on ultrasound images, Eur. Arch. Oto-Rhino-Laryngol. 274 (7) (2017) 1–7.
[11] J.-J. Ma, H. Ding, B.-H. Xu, C. Xu, L.-J. Song, B.-J. Huang, W.-P. Wang, Diagnostic performances of various gray-scale, color Doppler, and contrast-enhanced ultrasonography findings in predicting malignant thyroid nodules, Thyroid 24 (2) (2014) 355–363.
[12] H. Wu, Z. Deng, B. Zhang, Q. Liu, J. Chen, Classifier model based on machine learning algorithms: application to differential diagnosis of suspicious thyroid nodules via sonography, Am. J. Roentgenol. 207 (4) (2016) 859–864.
[13] A.A. Ardakani, A. Gharbali, A. Mohammadi, Classification of benign and malignant thyroid nodules using wavelet texture analysis of sonograms, J. Ultrasound Med. 34 (11) (2015) 1983–1989.
[14] A.A. Ardakani, A. Gharbali, A. Mohammadi, Application of texture analysis method for classification of benign and malignant thyroid nodules in ultrasound images, Iran. J. Cancer Prev. 8 (2) (2015) 116–124.
[15] S.-Y. Kim, E.-K. Kim, H.J. Moon, J.H. Yoon, J.Y. Kwak, Application of texture analysis in the differential diagnosis of benign and malignant thyroid nodules: comparison with gray-scale ultrasound and elastography, Am. J. Roentgenol. 205 (3) (2015) W343–W351.
[16] Y. Chang, A.K. Paul, N. Kim, J.H. Baek, Y.J. Choi, E.J. Ha, K.D. Lee, H.S. Lee, D. Shin, N. Kim, Computer-aided diagnosis for classifying benign versus malignant thyroid nodules based on ultrasound images: a comparison with radiologist-based assessments, Med. Phys. 43 (1) (2016) 554–567.
[17] U.R. Acharya, P. Chowriappa, H. Fujita, S. Bhat, S. Dua, J.E. Koh, L. Eugene, P. Kongmebhol, K.-H. Ng, Thyroid lesion classification in 242 patient population using Gabor transform features from high resolution ultrasound images, Knowl. Based Syst. 107 (2016) 235–245.
[18] M. Sollini, L. Cozzi, A. Chiti, M. Kirienko, Texture analysis and machine learning to characterize suspected thyroid nodules and differentiated thyroid cancer: where do we stand? Eur. J. Radiol. 99 (2018) 1–8.
[19] X. Sui, H.J. Liu, H.L. Jia, Q.M. Fang, Contrast-enhanced ultrasound and real-time elastography in the differential diagnosis of malignant and benign thyroid nodules, Exp. Ther. Med. 12 (2) (2016) 783–791.
[20] F. Zhang, X. Zhao, R. Han, M. Du, P. Li, X. Ji, Comparison of acoustic radiation force impulse imaging and strain elastography in differentiating malignant from benign thyroid nodules, J. Ultrasound Med. (2017) 1–11.
[21] P.W. Rosario, A.L.D. Silva, M.A.R. Borges, M.R. Calsolari, Is Doppler ultrasound of additional value to gray-scale ultrasound in differentiating malignant and benign thyroid nodules? Arch. Endocrinol. Metab. 59 (1) (2015) 79–83.
[22] A. Cavallo, D.N. Johnson, M.G. White, S. Siddiqui, T. Antic, M. Mathew, R.H. Grogan, P. Angelos, E.L. Kaplan, N.A. Cipriani, Thyroid nodule size at ultrasound as a predictor of malignancy and final pathologic size, Thyroid 27 (5) (2017) 641–650.
[23] S.A. Roman, J.A. Sosa, C.C. Solórzano, Management of Thyroid Nodules and Differentiated Thyroid Cancer: A Practical Guide, Springer, 2017.
[24] C. Cortes, V. Vapnik, Support-vector networks, Mach. Learn. 20 (3) (1995) 273–297.
[25] A.R. van Erkel, P.M.T. Pattynama, Receiver operating characteristic (ROC) analysis: basic principles and applications in radiology, Eur. J. Radiol. 27 (2) (1998) 88–94.
[26] J. Ophir, I. Cespedes, H. Ponnekanti, Y. Yazdi, X. Li, Elastography: a quantitative method for imaging the elasticity of biological tissues, Ultrason. Imaging 13 (2) (1991) 111–134.
[27] J. Xia, H. Chen, Q. Li, M. Zhou, L. Chen, Z. Cai, Y. Fang, H. Zhou, Ultrasound-based differentiation of malignant and benign thyroid nodules: an extreme learning machine approach, Comput. Methods Prog. Biomed. 147 (2017) 37–49.
[28] S.J. Nam, J. Yoo, H.S. Lee, E.-K. Kim, H.J. Moon, J.H. Yoon, J.Y. Kwak, Quantitative evaluation for differentiating malignant and benign thyroid nodules using histogram analysis of grayscale sonograms, J. Ultrasound Med. 35 (4) (2016) 775–782.
[29] J.K. Hoang, J.A. Sosa, X.V. Nguyen, P.L. Galvin, J.D. Oldan, Imaging thyroid disease: updates imaging approach, and management pearls, Radiol. Clin. North Am. 53 (1) (2015) 145–161.
[30] G.D. Soto, I. Halperin, M. Squarcia, F. Lomeña, M.P. Domingo, Update in thyroid imaging. The expanding world of thyroid imaging and its translation to clinical practice, Hormones (Athens) 9 (4) (2010) 287–298.